British Journal of Pharmacology

DOI:10.1111/j.1476-5381.2012.02232.x
www.brjpharmacol.org

RESEARCH PAPER

Modulation of K_v7 potassium channels by a novel opener pyrazolo[1,5-a]pyrimidin-7(4H)-one compound QO-58

F Zhang[1,2,3], Y Mi[1,2,3], JL Qi[4], JW Li[5], M Si[1,2,3], BC Guan[1,2,3], XN Du[1,2,3], HL An[5] and HL Zhang[1,2,3]

[1]*The Key Laboratory of Neural and Vascular Biology, Ministry of Education, Shijiazhuang, China,* [2]*The Key Laboratory of New Drug Pharmacology and Toxicology, Hebei Province, Shijiazhuang, China,* [3]*Department of Pharmacology, Hebei Medical University, Shijiazhuang, China,* [4]*Department of Development for New Drugs, School of Pharmacy, Hebei Medical University, Shijiazhuang, China, and* [5]*Institute of Biophysics, School of Sciences, Hebei University of Technology, Tianjin, China*

Correspondence
Professor Hailin Zhang or Dr Fan Zhang, Department of Pharmacology, Hebei Medical University, No. 361 East Zhongshan Road, Shijiazhuang, Hebei 050017, China. E-mail: zhanghl@hebmu.edu.cn; z.hailin@yahoo.com; zhangfanyaoli@yahoo.com.cn

Keywords
KCNQ/M-channel; PPOs; opener; neuropathic pain; QO-58; DRG

Received
17 May 2012
Revised
22 August 2012
Accepted
17 September 2012

BACKGROUND AND PURPOSE

Modulation of K_v7/M channel function represents a relatively new strategy to treat neuronal excitability disorders such as epilepsy and neuropathic pain. We designed and synthesized a novel series of pyrazolo[1,5-a] pyrimidin-7(4H)-one compounds, which activate K_v7 channels. Here, we characterized the effects of the lead compound, QO-58, on K_v7 channels and investigated its mechanism of action.

EXPERIMENTAL APPROACH

A perforated whole-cell patch technique was used to record K_v7 currents expressed in mammalian cell lines and M-type currents from rat dorsal root ganglion neurons. The effects of QO-58 in a rat model of neuropathic pain, chronic constriction injury (CCI) of the sciatic nerve, were also examined.

KEY RESULTS

QO-58 increased the current amplitudes, shifted the voltage-dependent activation curve in a more negative direction and slowed the deactivation of $K_v7.2/K_v7.3$ currents. QO-58 activated $K_v7.1$, $K_v7.2$, $K_v7.4$ and $K_v7.3/K_v7.5$ channels with a more selective effect on $K_v7.2$ and $K_v7.4$, but little effect on $K_v7.3$. The mechanism of QO-58's activation of K_v7 channels was clearly distinct from that used by retigabine. A chain of amino acids, $Val^{224}Val^{225}Tyr^{226}$, in $K_v7.2$ was important for QO-58 activation of this channel. QO-58 enhanced native neuronal M currents, resulting in depression of evoked action potentials. QO-58 also elevated the pain threshold of neuropathic pain in the sciatic nerve CCI model.

CONCLUSIONS AND IMPLICATIONS

The results indicate that QO-58 is a potent modulator of K_v7 channels with a mechanism of action different from those of known K_v7 openers. Hence, QO-58 shows potential as a treatment for diseases associated with neuronal hyperexcitability.

Abbreviations

BFNC, benign familial neonatal convulsions; CCI, chronic constriction injury; DRG, dorsal root ganglion; PPOs, pyrazolo[1,5-a] pyrimidin-7(4H)-ones; RTG, retigabine; SAR, structure-activity relationship

Introduction

The M-type K^+ channel plays an important role in controlling neuronal excitability (Hu *et al.*, 2007). It is now well established that the KCNQ gene family (K_v7) underlies the molecular basis of M currents (Wang *et al.*, 1998). Spontaneous mutations in K_v7 subunits cause epilepsy in humans and mice. In addition, K_v7 channels are expressed in the sensory system, such as the trigeminal ganglion neurons (Yoshida and Matsumoto, 2005) and dorsal root ganglion (DRG) (Linley *et al.*, 2008), and are possibly involved in migraine and neuropathic pain. Therefore, modulation of $K_v7.2/K_v7.3$ channels represents a new strategy for treating neuronal excitability disorders such as migraine, epilepsy and neuropathic pain (Dedek *et al.*, 2001; Munro and Dalby-Brown, 2007; Wuttke *et al.*, 2007).

Over the past few years, multiple compounds have been reported to activate K_v7 channels (Miceli *et al.*, 2008; Xiong *et al.*, 2008). The prototype activator of K_v7 channels is retigabine (Kapetanovic *et al.*, 1995). Retigabine activates $K_v7.2$, $K_v7.3$, $K_v7.4$ and $K_v7.5$ channels, but inhibits $K_v7.1$ channels (Tatulian *et al.*, 2001). A crucial Trp^{236} residue in the cytoplasmic part of S5 is believed to be important for retigabine-induced activation of $K_v7.2$ channels (Wuttke *et al.*, 2005). Zinc pyrithione (ZnPy) has been found to strongly potentiate all K_v7 channels except $K_v7.3$ (Xiong *et al.*, 2007). The key determinants of this effect of ZnPy include a leucine residue in S5 (Leu^{249}) and another one within the linker (Leu^{275}) between S5 and the pore region; these are different from retigabine's activation sites (Xiong *et al.*, 2008). Fenamates, including meclofenamic acid and diclofenac, currently used as non-steroidal anti-inflammatory drugs (NSAIDs), are another series of K_v7 channel activators (Peretz *et al.*, 2005). Diclofenac activates $K_v7.4$ but blocks $K_v7.5$ channels (Brueggemann *et al.*, 2011). Compounds NH6 and NH29 were synthesized based on the structural template of diclofenac (Peretz *et al.*, 2007). NH29 acts as a gating modifier and is targeted at the voltage sensor of $K_v7.2$ channels (Peretz *et al.*, 2010). Recently, we found that another NSAID drug, celecoxib, also interacts with the retigabine binding site to activate K_v7 channels (Du *et al.*, 2011).

Activators of K_v7 channels have been shown to have great potential for clinical applications. Retigabine has recently been found to be an effective treatment of epileptic diseases clinically (Fattore and Perucca, 2011; Weisenberg and Wong, 2011). Noticeably, retigabine also has analgesic effects, especially in animal models of chronic inflammatory (Linley *et al.*, 2008; Liu *et al.*, 2008) and neuropathic pain (Blackburn-Munro and Jensen, 2003; Rose *et al.*, 2011). In addition, flupirtine, an analogue of retigabine, is also a potent K_v7 channel activator. Encouragingly, flupirtine is already used as a centrally acting, non-opioid analgesic for the treatment of a variety of pain states (Devulder, 2010).

In an effort to find new chemical structures of K_v7/M-channel openers, we designed and synthesized a novel series of pyrazolo[1,5-a] pyrimidin-7(4H)-one compounds (PPOs), which have the ability to open K_v7 channels (Jia *et al.*, 2011; Qi *et al.*, 2011). We evaluated and analysed the effects of about 120 analogues of PPOs on $K_v7.2/K_v7.3$ channels to construct a structure-activity relationship (SAR). From this SAR study, we found that a trifluoromethyl group at the 2-position is required for this activity; at the 3-position, substitution with a phenyl or naphthyl group afforded best activity and electron withdrawing substitutes on the aromatic ring at the 5-position is the most important site for activity. The optimization of PPOs based on the SAR results produced the lead compound QO-58, which showed the best EC_{50} (0.06 ± 0.01 μM) for activation of $K_v7.2/K_v7.3$ (Qi *et al.*, 2011). In the present study, we characterized the effects of QO-58 on K_v7 channels using whole-cell patch-clamp recording techniques (Figure 1A). Our results indicate that QO-58 is a potent activator of K_v7 channels with a mechanism of action different from those of known K_v7 openers. QO-58 also has the potential to be developed as a treatment for diseases associated with neuronal hyperexcitability.

Methods

Compounds

QO-58 and retigabine (Purity >98% by HPLC-DAD) were synthesized in the Department of New Drugs Development, School of Pharmacy, Hebei Medical University, and their purity was verified by MS and NMR analysis (Qi *et al.*, 2011). XE991 was purchased from Sigma (St Louis, MO, USA).

DNA constructs

Plasmids encoding human $K_v7.1$, human $K_v7.2$, rat $K_v7.3$, human $K_v7.4$ and human $K_v7.5$ (GenBank accession numbers: NM000218, AF110020, AF091247, AF105202 and AF249278, respectively) were kindly provided by Diomedes E. Logothetis (Virginia Commonwealth University, Richmond, VA, USA). $K_v7.2$ (R207W), $K_v7.2$ (L275A), $K_v7.2$ (Y284C), $K_v7.2$ (A306T) and $K_v7.2$ (W236L) mutants were kindly provided by Zhaobing Gao (Chinese Academy of Sciences, Shanghai, China). $K_v7.2$ (VVY224225226AIC) mutants were produced by *Pfu* DNA polymerase with a QuickChange kit (Stratagene, La Jolla, CA, USA). The structure of the mutants was confirmed with DNA sequencing.

The nomenclature of K_v7 potassium channels and other receptors and channels conforms to BJP's *Guide to Receptors and Channels* (Alexander *et al.*, 2011).

Cell culture

Stable CHO cells expressing $K_v7.2/7.3$ channels (a kind gift from Professor Wang Kewei, Peking University) were grown in DMEM supplemented with 10% fetal calf serum, 1× non-essential amino acids, 600 $\mu g \cdot mL^{-1}$ G418 and 600 $\mu g \cdot mL^{-1}$ hygromycin B.

HEK293 cells were cultured in DMEM supplemented with 10% fetal calf serum and antibiotics. For transfection of 8 wells of cells, a mixture of 4 μg K_v7, 4 μg RFP pcDNAs and 6 μL Lipofectamine 2000 reagent (Invitrogen, Carlsbad, CA, USA) was prepared in 1.2 mL DMEM. The mixture was then applied to the cell culture wells and incubated for 4–6 h. Recordings were made 24 h after cell transfection, and the cells were used within 48 h.

Rat DRG neuron culture

DRGs were extracted from the intervertebral foramina of 7-day-old Sprague-Dawley rats (provided by Experimental

Animal Center of Hebei Province). A total of 40 adult male Sprague-Dawley rats were used in our study. The ganglia were digested at 37°C with 1 mg·mL^{-1} collagenase for 30 min, followed by another 30 min digestion with 2.5 mg·mL^{-1} trypsin. They were subsequently suspended at least twice in DMEM plus 10% fetal calf serum to stop digestion. Thereafter, the ganglia were plated on poly-D-lysine-coated glass coverslips. The neurons were cultured for 4 days and used within 48 h.

The results of all studies involving animals are reported in accordance with the ARRIVE guidelines for reporting experiments involving animals (Kilkenny *et al.*, 2010; McGrath *et al.*, 2010).

Electrophysiology

For current measurements in the CHO cell, HEK293 cells and DRG neurons, recordings were performed using the perforated (amphotericin B, 250 μg·mL^{-1}, Sigma) patch-clamp technique at room temperature. The signals were amplified using an HEAK EPC10 patch-clamp amplifier. The acquisition rate was 10 kHz and signals were filtered at 2.5 kHz. Patch electrodes were pulled with a micropipette puller (Sutter Instruments, Novato, CA, USA) and fire polished to a final resistance of 1–2 MΩ. Series resistances were compensated by 60–80%. The internal and external solution for the mammalian cell lines and rat DRG neuron recording was as follows (in mM): KCl 150, $MgCl_2$ 5, HEPES 10, pH 7.4 adjusted with KOH; NaCl 160, KCl 2.5, $MgCl_2$ 1, $CaCl_2$ 2, glucose 10, HEPES 20 and pH 7.4 adjusted with NaOH respectively.

Neuropathic pain model of sciatic nerve chronic constriction injury

Adult male Sprague-Dawley rats (weighing 160~180 g, provided by Experimental Animal Center of Hebei Province) were used in this experiment. The use of animals in this study was approved by the Animal Care and Ethical Committee of Hebei Medical University (Shijiazhuang, China), under the IASP guidelines for animal use. The rats were kept in plastic cages in a room with a temperature of 22–25°C, under 12/12 h light/dark cycle (lights on from 7 h to 19 h). Food and water were available *ad libitum*. The operation procedures for establishing the neuropathic pain model with sciatic nerve chronic constriction injury (CCI) have been described previously (Sommer and Schafers, 1998). Briefly, the rats were anaesthetized with an i.p. injection of sodium pentobarbital (10–20 mg kg^{-1}). The depth of anaesthesia was assessed by responses to the pinching of the rats legs; no response to the pinching was taking as the sign for further operation.

Four ligatures (chromic catgut 4-0) were placed around the nerve with a distance of 1 mm between each ligature. The ligatures were loosely tied until a short flick of the ipsilateral hind limb was observed. The rats with above operation were divided into five groups with eight animals in each group: control solvent (17% PEG400) group, 12.5 mg·kg^{-1} retigabine group, and three QO-58 groups with different doses of 12.5 mg·kg^{-1}, 25 mg·kg^{-1} and 50 mg·kg^{-1}. Drugs were given by i.p. injection twice a day. Mechanical and heat nociceptive threshold was assessed before and after performing surgery on days 1, 3, 5, 7, 9, 11 and 19.

Mechanical test

Response threshold to mechanical stimulus was assessed as described previously (Chaplan *et al.*, 1994). Briefly, calibrated nylon filaments (Von Frey hair, Stoelting Co, Chicago, IL, USA) with different bending forces were applied to the mid-plantar surface of the right hind paw of the rats. The filaments were applied starting with the softest and continuing in ascending order of stiffness. A brisk withdrawal of the right hind limb was considered a positive response.

Radiant heat test

Response to heat stimulus was tested on the right hind paw of the rats using a radiant heat lamp source (Hargreaves *et al.*, 1988). The intensity of the radiant heat stimulus was maintained at 25 ± 0.1°C. Response of right hind paw withdrawal threshold (elapse time) was noted.

Data analysis and statistics

The concentration-response curve was fitted by logistic equation: $y = A_2 + (A_1 - A_2)/(1+(x/x_0)^{n_H})$, where x is the drug concentration, and n_H is the Hill coefficient. The current activation curves were generated by plotting the normalized tail current amplitudes against the step potentials and were fitted with a Boltzmann equation: $y = A/\{1 + \exp[(V_h - V_m)/k]\}$, where A is the amplitude of relationship, V_h is the voltage for half-maximal activation, V_m is the test potential and k is the slope factor of the curve. The activation and deactivation traces were fitted to a single exponential function: $I = A \times [1 - \exp(-t/\tau)]$, where I is the current, A is amplitudes, t is time and τ is the time constant. Results are expressed as means ± SEM. Statistical analysis of differences between groups was carried out using Student's *t*-test or paired *t*-test. *P*-values ≤0.05 were considered significant.

Results

The effects of compound QO-58 on expressed $K_v7.2/K_v7.3$ currents

We first studied the effect of compound QO-58 (Figure 1A) on the activation of $K_v7.2/K_v7.3$ channels stably expressed in CHO cells. Superfusion of the cells with 3 μM QO-58 increased both the activated stead state current (–40 mV) and the deactivating tail current (–120 mV) amplitudes of $K_v7.2/K_v7.3$ channels (Figure 1B). Figure 1C shows the concentration-dependent effects of QO-58 on $K_v7.2/K_v7.3$ currents elicited by the depolarization potential of –40 mV. We then constructed a concentration-response relationship for the effects of QO-58 on $K_v7.2/K_v7.3$ currents (Figure 1D). QO-58 (100 μM) induced a maximal 6.15 ± 0.76-fold increase in the $K_v7.2/K_v7.3$ currents recoded at –40 mV. The current increase produced by 100 μM QO-58 was taken as the E_{max}, which was used to normalize the increase in $K_v7.2/K_v7.3$ currents produced by all concentrations of QO-58. The normalized concentration-response curves were fitted by a modified logistic equation, and the EC_{50} value was 2.3 ± 0.8 μM and the Hill coefficient was 0.6 ± 0.1 (Figure 1D) (n = 6).

Next, we studied the effect of compound QO-58 on voltage-dependent activation of $K_v7.2/K_v7.3$ currents. Super-

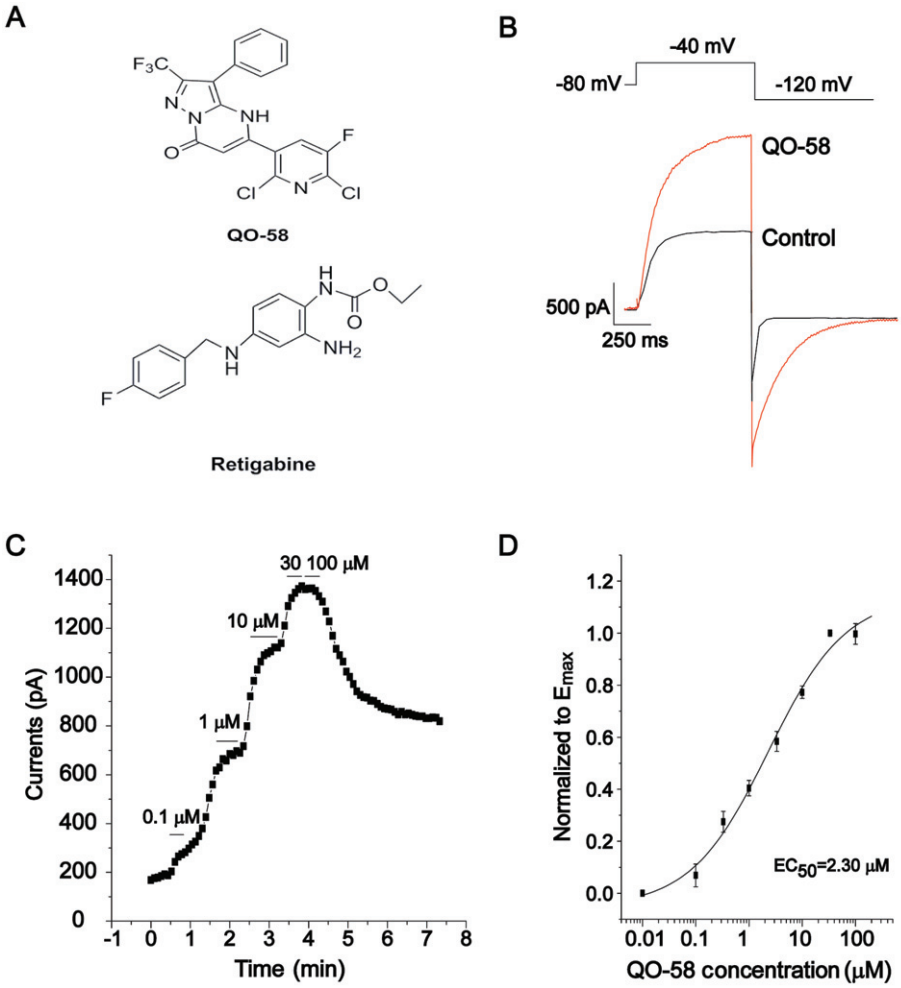

Figure 1

Compound QO-58 enhances $K_v7.2/K_v7.3$ channel currents. (A) The structure of compound QO-58 and retigabine. (B) Typical outward currents elicited by step depolarization to –40 mV from a holding potential of –80 mV in the absence and presence of 3 μM QO-58. (C) QO-58 concentration-dependently increased $K_v7.2/K_v7.3$ channel currents generated at –40 mV. (D) QO-58-induced outward currents were normalized to the maximal effect (E_{max}) value and fit to a logistic function; EC_{50} value was 2.3 ± 0.8 μM and the slope factor was 0.6 ± 0.1 (n = 6).

fusion of the cells with 0.3, 1 and 3 μM QO-58 increasingly shifted the threshold for channel activation to more hyperpolarized potentials (Figure 2A). Tail current amplitudes at –120 mV resulting from different test potentials were normalized and fitted by the Boltzmann function. QO-58 concentration-dependently shifted the $V_{1/2}$ of $K_v7.2/K_v7.3$ currents to more negative potentials, the EC_{50} value was 1.2 ± 0.2 μM and the Hill coefficient was 1.2 ± 0.3 (n = 6) (Figure 2B,C).

Then we studied the effects of QO-58 on the kinetics of $K_v7.2/K_v7.3$ currents. The activation and deactivation currents were both fitted to a single exponential function. Application of 10 μM QO-58 significantly slowed channel activation and deactivation kinetics (Figure 2D,E).

Selectivity of compound QO-58 on K_v7 channels

The K_v7 family of potassium channels consists of five subtypes, $K_v7.1$ to $K_v7.5$ (Ng *et al.*, 2011). We studied the selectivity of QO-58 on K_v7 channels expressed in HEK293 cell. $K_v7.5$ did not produce significant currents when expressed alone, thus $K_v7.5$ was co-expressed with $K_v7.3$ and the effect of QO-58 was tested on the heterologous $K_v7.3/K_v7.5$ currents. When K_v7 currents were recorded at –40 mV, QO-58 (10 μM) significantly increased the $K_v7.1$, $K_v7.2$, $K_v7.4$ and $K_v7.3/K_v7.5$ currents, but only slightly increased $K_v7.3$ currents (Figure 3B).

QO-58 concentration-dependently increased $K_v7.1$, $K_v7.2$, $K_v7.4$ and $K_v7.3/K_v7.5$ channel currents recorded at –40 mV; the EC_{50} values for QO-58 were 7.0 ± 1.0, 1.3 ± 1.0, 0.6 ± 0.1 and 5.2 ± 2.2 μM for $K_v7.1$, $K_v7.2$, $K_v7.4$ and $K_v7.3/K_v7.5$ channels, respectively (Figure 4). Thus, QO-58 is more potent at activating $K_v7.2$ and $K_v7.4$ channels than the other channels. QO-58 (10 μM) produced a substantial leftward shift of the $V_{1/2}$ of $K_v7.1$, $K_v7.2$, $K_v7.4$ and $K_v7.3/K_v7.5$ currents by 21.7 ± 1.1 mV (n = 7), 56.8 ± 5.4 mV (n = 6), 58.7 ± 2.9 mV (n = 6) and 47.4 ± 2.8 mV (n = 5), respectively; on the other hand, the $V_{1/2}$ of $K_v7.3$ was shifted to the right by 2.7 ± 0.1 mV. (Figure 5 and Table 1) (n = 5).

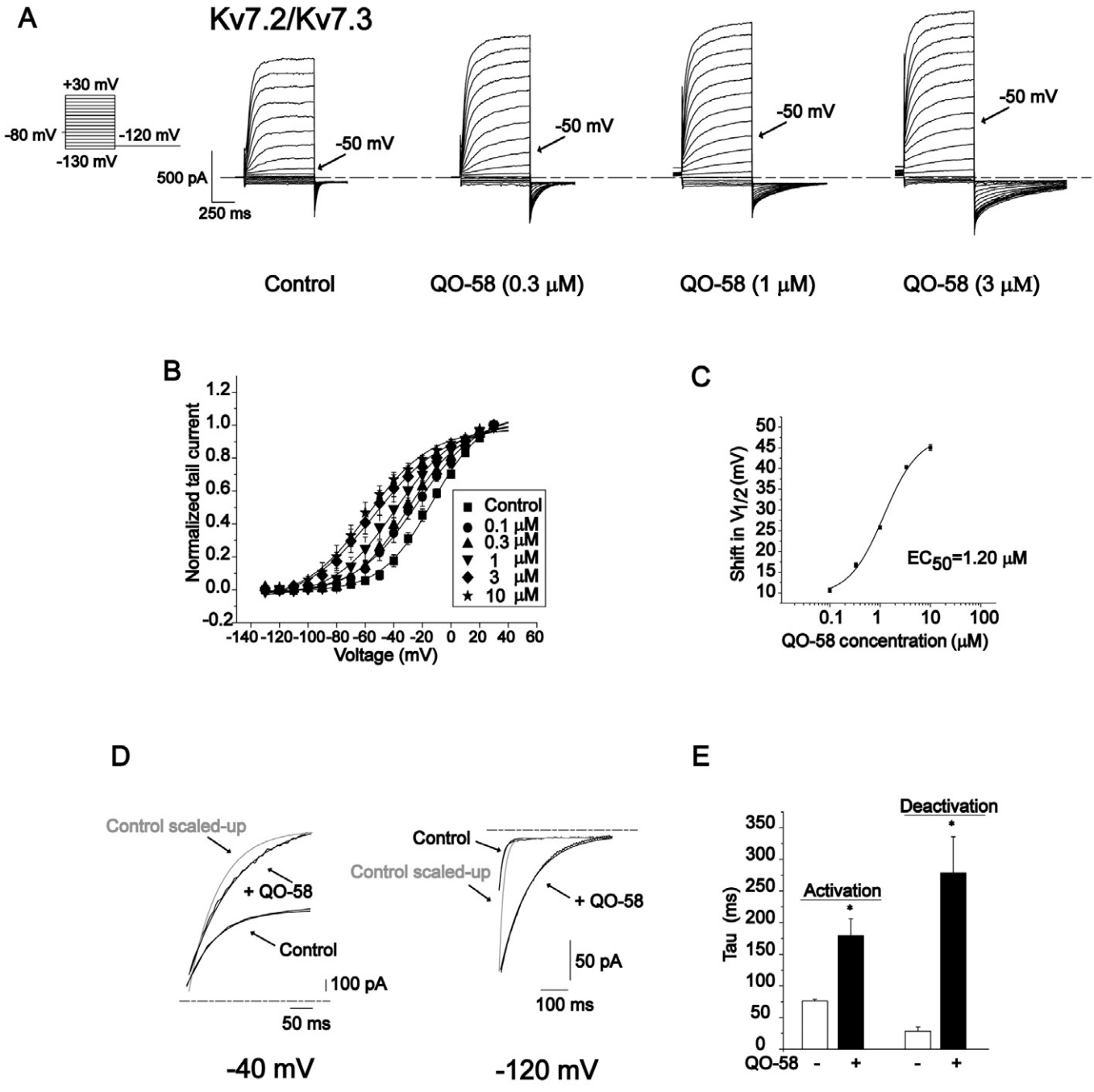

Figure 2

Compound QO-58 shifts the voltage-dependence of $K_v7.2/K_v7.3$ channel activation. (A) Series of outward currents elicited by depolarizing voltage steps (hold at –80 mV, in 10 mV incremental voltage steps from –130 to +30 mV) with increasing concentrations of QO-58. (B) The activation curves were generated in the absence of QO-58(■), and in the presence of 0.1 μM, 0.3 μM, 1 μM, 3 μM, 10 μM QO-58. (C) The magnitude of the QO-58-induced shifts in $V_{1/2}$ ($\Delta V_{1/2}$, towards more negative potentials) was calculated and plotted against QO-58 concentration; EC_{50} value was 1.2 ± 0.2 μM and a slope factor was 1.2 ± 0.3 ($n = 6$). (D) The effects of QO-58 on the activation and deactivation kinetics of $K_v7.2/K_v7.3$ currents. (E) Summary for results depicted in (D) ($n = 5$, $^*P < 0.05$).

QO-58 (10 μM) significantly slowed the activation kinetics of $K_v7.4$ and $K_v7.3/K_v7.5$ currents, and slowed the deactivation kinetics of K_v7 currents. It was noteworthy that QO-58 largely increased the deactivation time constant of $K_v7.2$ by 6.2-fold, and greatly increased the deactivation time constant of $K_v7.4$ by 36.4-fold (Supporting Information Figure S1 and Table 2) ($n = 5$–7).

In all, QO-58 was found to be a potent K_v7 channel opener with more selective effect on $K_v7.2$ and $K_v7.4$ channels, but has a minor effect on the $K_v7.3$ channel.

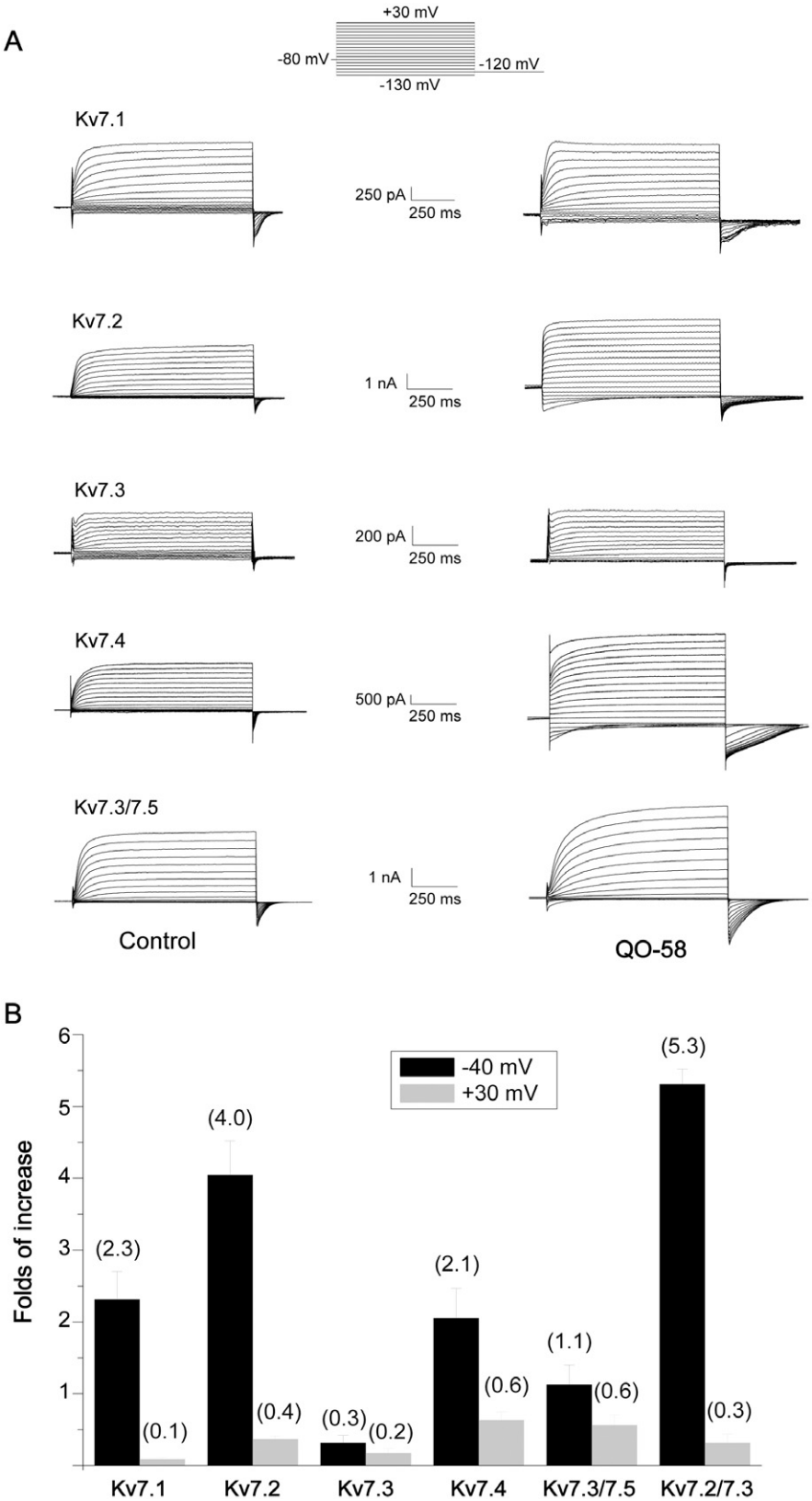

Figure 3

Compound QO-58 enhances K_v7 channel currents. (A) Whole-cell currents with K_v7 channel in the absence (left panels) and presence (right panels) of 10 μM QO-58. (B) Histogram plotting of the QO-58 effect on K_v7 channel currents generated by step depolarization at –40 mV and at +30 mV (n = 5–8).

The mechanism for QO-58 activation of K_v7 currents

The Trp^{236} residue in $K_v7.2$ is believed to be a key amino acid in mediating the activation by retigabine, thus mutation of tryptophan to leucine [$K_v7.2$ (W236L)] renders the channel insensitive to retigabine (Wuttke *et al.*, 2005). Hence, we studied the effect of QO-58 on this mutant $K_v7.2$ (W236L). As shown in Figure 6C,D, QO-58 (10 μM) still markedly enhanced the $K_v7.2$ (W236L) currents (the currents were increased by 1.6 ± 0.4-folds at –50 mV) in this mutant channel and induced a leftward shift of the activation curve, with $V_{1/2}$ changed as effectively as in the wild-type $K_v7.2$ (n = 5, $P < 0.05$). These data suggest that QO-58 does not share the same mechanism of action as retigabine for activation of K_v7 currents (Wuttke *et al.*, 2005).

As it was found that QO-58 enhances all the K_v7 channel currents except $K_v7.3$ (Figure 3), we compared the sequences of these K_v7 channels and found that $Val^{224}Val^{225}Tyr^{226}$ inside the S4 and S5 segments of the K_v7 were conserved in $K_v7.1$, $K_v7.2$, $K_v7.4$ and $K_v7.5$, while in $K_v7.3$ these residues were Ala-Ile-Cys. Thus, we made and tested a mutant $K_v7.2$ [VVY224,225,226AIC ($K_v7.2$ (AIC)]; compared with the wild-type $K_v7.2$ channel, $K_v7.2$ (AIC) had two major different features. Firstly, $K_v7.2$ (AIC) currents demonstrated a prominent inactivation (Figure 6E); secondly, the voltage-dependent activation of $K_v7.2$ (AIC) was greatly shifted to a more negative potential, and the $V_{1/2}$ was now –81.0 ± 2.2 mV. QO-58 (10 μM) abolished the inactivation and did not affect the steady-state current amplitude of $K_v7.2$ (AIC). On the other

Table 1

The maximal changes of $V_{1/2}$ of Kv7 subtype currents induced by QO-58 (10 μM)

	$V_{1/2}$ (mV) (control)	$V_{1/2}$ (mV) (QO-58)	$\Delta V_{1/2}$ (mV)
$K_v7.1$	–17.8 ± 0.8	–39.5 ± 1.1	21.7 ± 1.1
$K_v7.2$	–18.1 ± 1.9	–74.9 ± 5.4	56.8 ± 5.4
$K_v7.3$	–32.4 ± 3.1	–35.1 ± 2.1	2.7
$K_v7.4$	–22.0 ± 1.4	–80.7 ± 2.9	58.7 ± 2.9
$K_v7.2/K_v7.3$	–13.2 ± 1.1	–58.3 ± 1.7	45.1 ± 1.7
$K_v7.3/K_v7.5$	–35.5 ± 2.4	–51.7 ± 2.8	47.2 ± 2.8

All values are mean ± SEM (n = 5–7). $\Delta V_{1/2}$ means the difference between $V_{1/2}$ of control and that of compound.

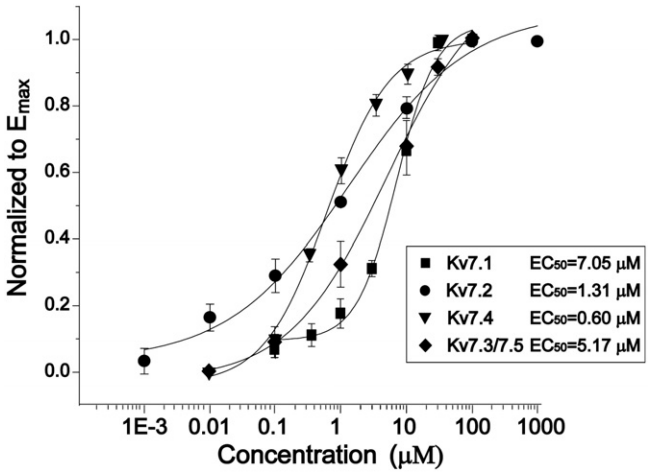

Figure 4

Concentration-dependent effects of QO-58 on K_v7 channel currents. The currents were measured at –40 mV. The concentration-response relationships were fitted with the logistic function (n = 5–8).

Table 2

The effects of QO-58 on channels activation and deactivation kinetics of K_v7 subtypes

		Time constants (ms)	
		Control	QO-58 (10 μM)
$K_v7.1$	Activation τ (–40 mV)	122.5 ± 22.8	175 ± 35.9
	Deactivation τ (–120 mV)	31.2 ± 2.3	84.2 ± 26.8
$K_v7.2$	Activation τ (–40 mV)	96.6 ± 12.0	137.6 ± 13.4
	Deactivation τ (–120 mV)	15 ± 1.5	96.4 ± 12.5
$K_v7.3$	Activation τ (–40 mV)	166.3 ± 25.7	175 ± 18.9
	Deactivation τ (–120 mV)	18.5 ± 3.0	29.3 ± 4.2
$K_v7.4$	Activation τ (–40 mV)	34.4 ± 4.4	100.5 ± 3.9
	Deactivation τ (–120 mV)	8.7 ± 0.2	316.6 ± 125.8
$K_v7.2/K_v7.3$	Activation τ (–40 mV)	76.0 ± 2.5	179.5 ± 26.4
	Deactivation τ (–120 mV)	28.3 ± 6.8	278.5 ± 57.3
$K_v7.3/K_v7.5$	Activation τ (–40 mV)	83 ± 16.6	137 ± 19.6
	Deactivation τ (–120 mV)	32.1 ± 1.8	253.2 ± 61.9

All values are mean ± SEM (n = 4–7).

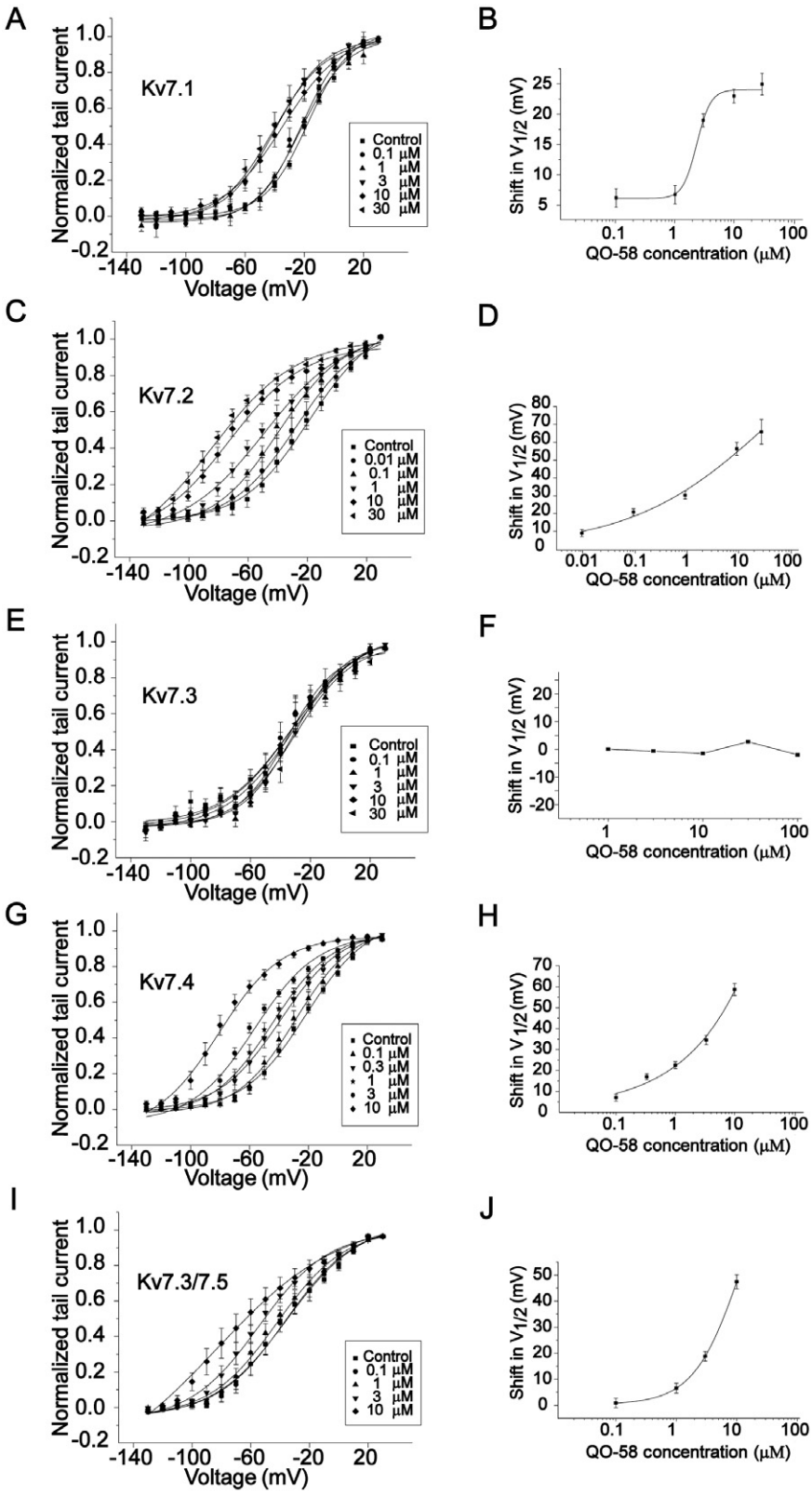

Figure 5

Concentration-dependent effects of QO-58 on the voltage-dependent activation of K_v7 channel currents. The left panels (A,C,E,G,I) show activation curves for K_v7 currents generated from tail currents with increasing concentrations of QO-58. The right panels (B,D,F,H,J) show the magnitude of the QO-58-induced shifts in $V_{1/2}$ calculated and plotted against QO-58 concentration (n = 5–7).

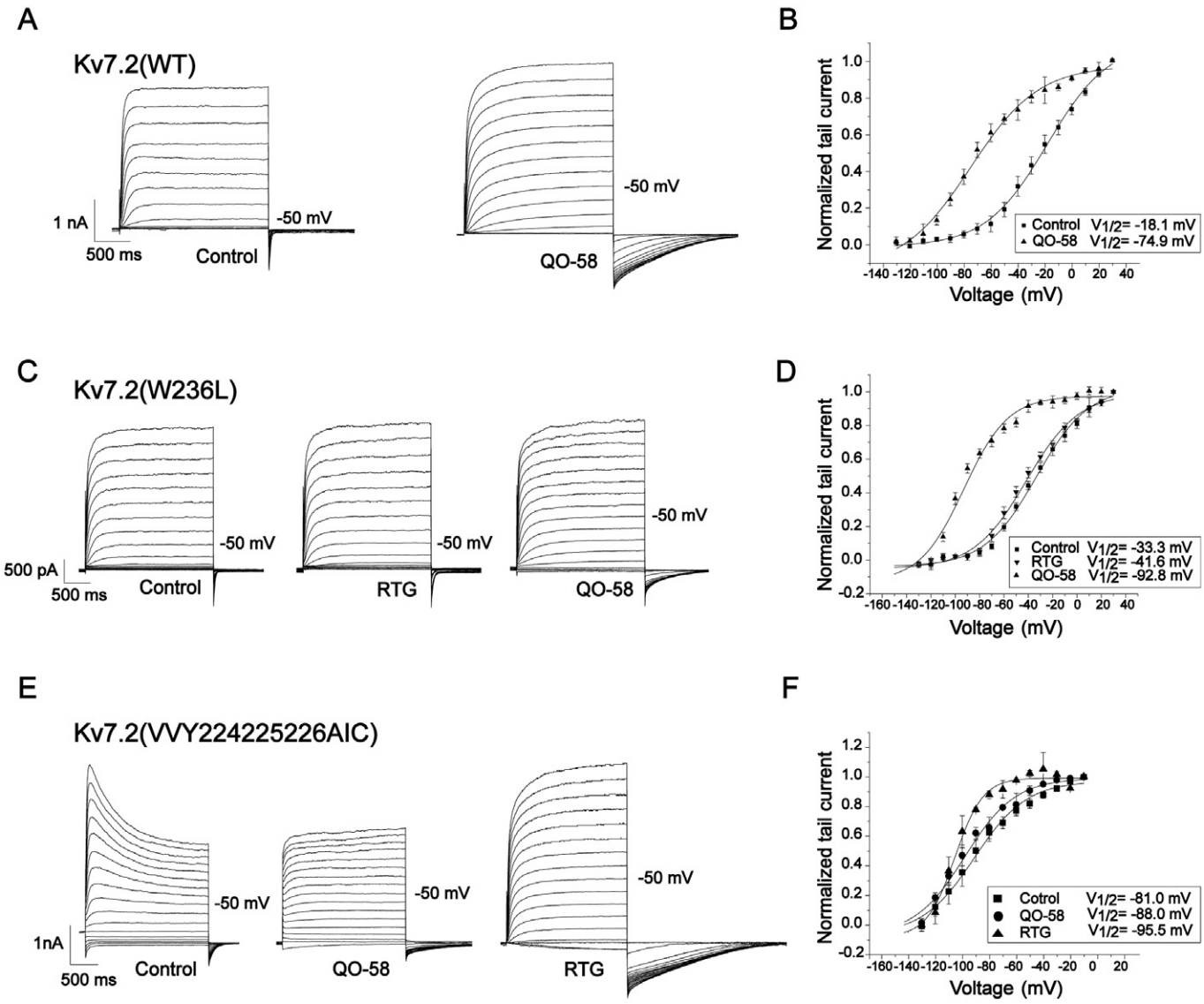

Figure 6

The effect of QO-58 on wild-type $K_v7.2$, $K_v7.2$ (W236L) and $K_v7.2$ (AIC) channel currents. (A) The $K_v7.2$ currents were elicited by a series of depolarizing voltage steps from –130 to +30 mV from a holding potential of –120 mV in the absence and presence of 10 μM QO-58. (B) QO-58 induced a leftward shift of the activation curve from $V_{1/2}$ = –18.1 ± 1.9 mV to $V_{1/2}$ = –74.9 ± 5.4 mV. (C,D) The effects of QO-58 and RTG on $K_v7.2$ (W236L) currents. QO-58 and RTG induced a leftward shift of the activation curve from $V_{1/2}$ = –33.3 ± 1.7 mV to $V_{1/2}$ = –92.8 ± 2.7 mV and –41.6 ± 2.0 mV respectively (n = 5). (E,F) The effects of QO-58 and RTG on $K_v7.2$ (AIC) currents. QO-58 and RTG induced a leftward shift of the activation curve from $V_{1/2}$ = –81.0 ± 2.2 mV to $V_{1/2}$ = –88.0 ± 2.1 mV and –95.5 ± 1.7 mV respectively (n = 5).

hand, RTG (10 μM) also abolished the inactivation but more importantly increased greatly the steady-state current amplitude of $K_v7.2$ (AIC) (Figure 6E). Similarly, QO-58 was significantly less effective than RTG in further hyperpolarizing the voltage-dependent activation of $K_v7.2$ (AIC) (Figure 6F). These results indicate that $Val^{224}Val^{225}Tyr^{226}$ in $K_v7.2$ are involved in QO-58 activation of K_v7 channels, and also further suggest that QO-58 and RTG activate $K_v7.2$ channel using a different mechanism.

We made further efforts to identify the amino acids in $K_v7.2$ possibly involved in the activity of QO-58. We constructed a docking simulation model for the interaction of QO-58 with residues within S5 and S6 of the $K_v7.2$ channel (Supporting Information Figure S2), a procedure we have used in our previous work (Du *et al.*, 2011). Two residues, Aal^{306} and Leu^{275} in $K_v7.2$, were identified for possibly interacting with QO-58. We then tested the effects of QO-58 on $K_v7.2$ (A306T) and $K_v7.2$ (L275A) mutants (Supporting Information Figure S3). Two things are clear from these results. Firstly, the potentiating effects of QO-58 on the maximum current amplitude of $K_v7.2$ were converted to an inhibitory effect in $K_v7.2$ (A306T). Secondly, the effects of QO-58 on the voltage-dependent activation of $K_v7.2$ were greatly reduced; a change in $V_{1/2}$ of 56.8 mV by QO-58 was seen for $K_v7.2$, and

a change of 28.5 mV was seen for $K_v7.2$ (A306T) and 37.3 mV for $K_v7.2$ (L275A). These results suggest that alanine 306 and leucine 275 in K_v7 could also be important for mediating the activation of the K_v7 channels by QO-58.

Mutation on $K_v7.2$ and $K_v7.3$ channel can lead to benign familial neonatal convulsions (BFNCs) (Coppola *et al.*, 2003; Zhou *et al.*, 2006). We tested the effect of QO-58 on two of these mutants: $K_v7.2$ (R207W) and $K_v7.2$ (Y284C). Interestingly, QO-58 activated both $K_v7.2$ (R207W) and $K_v7.2$ (Y284C) mutants. These results indicate that QO-58 may be beneficial for treating benign familial neonatal convulsions (Supporting Information Figure S4).

QO-58 enhances the native M current in rat DRG neurons

We next examined the potential effect of QO-58 on native M-type K^+ currents in rat DRG neurons. M currents were activated by a depolarizing voltage of –20 mV, and tail M currents were observed at –60 mV (Figure 7A). Both QO-58 and RTG increased M currents by approximately 25% at 10 μM (Figure 7B). QO-58 also induced significant hyperpolarization of the resting membrane potential (RMP) to about –18.4 mV. Application of an M-channel antagonist, XE991, completely abolished the membrane hyperpolarization induced by QO-58 (Figure 7C,D). A perfusion of QO-58 immediately abolished the repetitive firing spikes from a DRG neuron (Figure 7E).

QO-58 elevated the threshold of neuropathic pain in the CCI model

A CCI of the sciatic nerve model was successfully established. The rats operated on to create CCI of the sciatic nerve displayed significantly reduced withdrawal threshold for mechanical stimulus and shortened withdrawal latency to thermal stimulus, from day 1 after the operation (Figure 8A,B). QO-58 and retigabine significantly increased the threshold of the mechanical stimulus 1–19 days after the operation. QO-58 concentration-dependently prolonged the withdrawal latency for a response to the thermal stimulus, and in the 50 $mg \cdot kg^{-1}$ QO-58 groups the withdrawal latency was prolonged to its pre-operation level.

Discussion and conclusions

Chemical modulators of K_v7 channels have become candidates for the treatment of diseases related to neuronal hyperexcitability. In addition, K_v7 channel modulators are also valuable probes for elucidating the channel gating mechanisms and their functional roles. In this study, we demonstrated that the compound QO-58, which we recently developed, is a potent modulator of the K_v7 channels. Importantly, QO-58 activated K_v7 channels with a mechanism clearly distinct from that used by retigabine.

Two outstanding features can be deduced from the observed effects of QO-58 on K_v7 currents. The first is a marked shift in the voltage-dependent activation of some K_v7 channels towards a more negative potential; the $V_{1/2}$ for $K_v7.2$, $K_v7.4$, $K_v7.2/K_v7.3$, $K_v7.3/K_v7.5$ were shifted about –40~–60 mV, whereas the $V_{1/2}$ for $K_v7.1$ was shifted about –20 mV, whereas the $V_{1/2}$ for $K_v7.3$ was not affected (Table 1). This effect of QO-58 has important implications. The negative shift of the voltage-dependent activation of K_v7 channel would lower the membrane potential threshold for K_v7 activation and thus would inevitably hyperpolarize the membrane potential, which would reduce the excitability of the cells expressing K_v7 channels. The above notion was well manifested in the effects of QO-58 action on DRG neurons: QO-58 significantly shifted the resting membrane potential of DRG neurons to a hyperpolarization potential and greatly reduced the firing spikes of these neurons (Figure 7). As $K_v7.2/K_v7.3$ (Wang *et al.*, 1998) and $K_v7.3/K_v7.5$ (Shah *et al.*, 2002) have been shown to underlie the neuronal M-type currents, these results corroborate the effects of QO-58.

The second outstanding feature of the effects of QO-58 on K_v7 is the significant slowing of the K_v7 deactivation kinetics. Although QO-58 also slowed the activation kinetics of K_v7, the effects on the deactivation kinetics were much stronger. Again, the efficacy of QO-58 on slowing the channel deactivation followed the same order as that found to shift the voltage-dependent activation of the different K_v7 subtypes; namely, the effects were greater on $K_v7.2$, $K_v7.4$, $K_v7.2/K_v7.3$, $K_v7.3/K_v7.5$ channels, but were less on $K_v7.1$, and were negligible on $K_v7.3$ (Table 2). As both the activation and the deactivation of K_v7 channel were slowed by QO-58, and slowing of channel activation would reduce the channel activity, it must be that the slowing of the channel deactivation by QO-58 contributed to the overall enhancement of the K_v7 channel. Thus the K_v7 channel became difficult to close in the presence of QO-58.

On the other hand, the effects of QO-58 on the amplitudes of K_v7 were less striking. Although QO-58 markedly enhanced the current amplitudes of K_v7 at negative membrane potentials (such as those at –40, –50 mV), it had much less effect on the maximal saturating current amplitudes recorded at more positive potentials; in fact, in the presence of QO-58, the current amplitudes at +30 mV were only increased by about 20–60% (Figure 3B).

It is clear that QO-58 uses a different mechanism from RTG to activate K_v7 channels. A tryptophan (W236) in $K_v7.2$ is the key determinant for the activation of $K_v7.2$ by RTG (Wuttke *et al.*, 2005). Clearly, Trp^{236} in $K_v7.2$ did not mediate the activation of $K_v7.2$ by QO-58, as QO-58 activated $K_v7.2$ (W236L) as effectively as wild-type $K_v7.2$ (Figure 6). Also, in contrast to RTG (Tatulian *et al.*, 2001) but similar to ZnPy (Xiong *et al.*, 2007), QO-58 had little effect on $K_v7.3$. $Val^{224}Val^{225}Tyr^{226}$ are conserved in all K_v7 except $K_v7.3$. Further, the mutant $K_v7.2$ (VVY224 225,226AIC) was not activated by QO-58 but still activated by RTG. These results suggest that $Val^{224}Val^{225}Tyr^{226}$ in $K_v7.2$ play an important role in the activation of K_v7 channels by QO-58. However, these results should be interpreted with caution; the properties of $K_v7.2$ (AIC) currents greatly changed compared with those of $K_v7.2$ (Figure 6), as the channel currents became inactive and the voltage-dependent activation was greatly shifted to the more negative potentials. It is not clear whether these changes affect the effects of QO-58 in an allosteric manner. Nevertheless, the finding that this $K_v7.2$ (AIC) was still activated by RTG suggests that $Val^{224}Val^{225}Tyr^{226}$ in $K_v7.2$ is indeed important for QO-58 activation of K_v7. With the help of docking modelling, we found that the mutation of $K_v7.2$

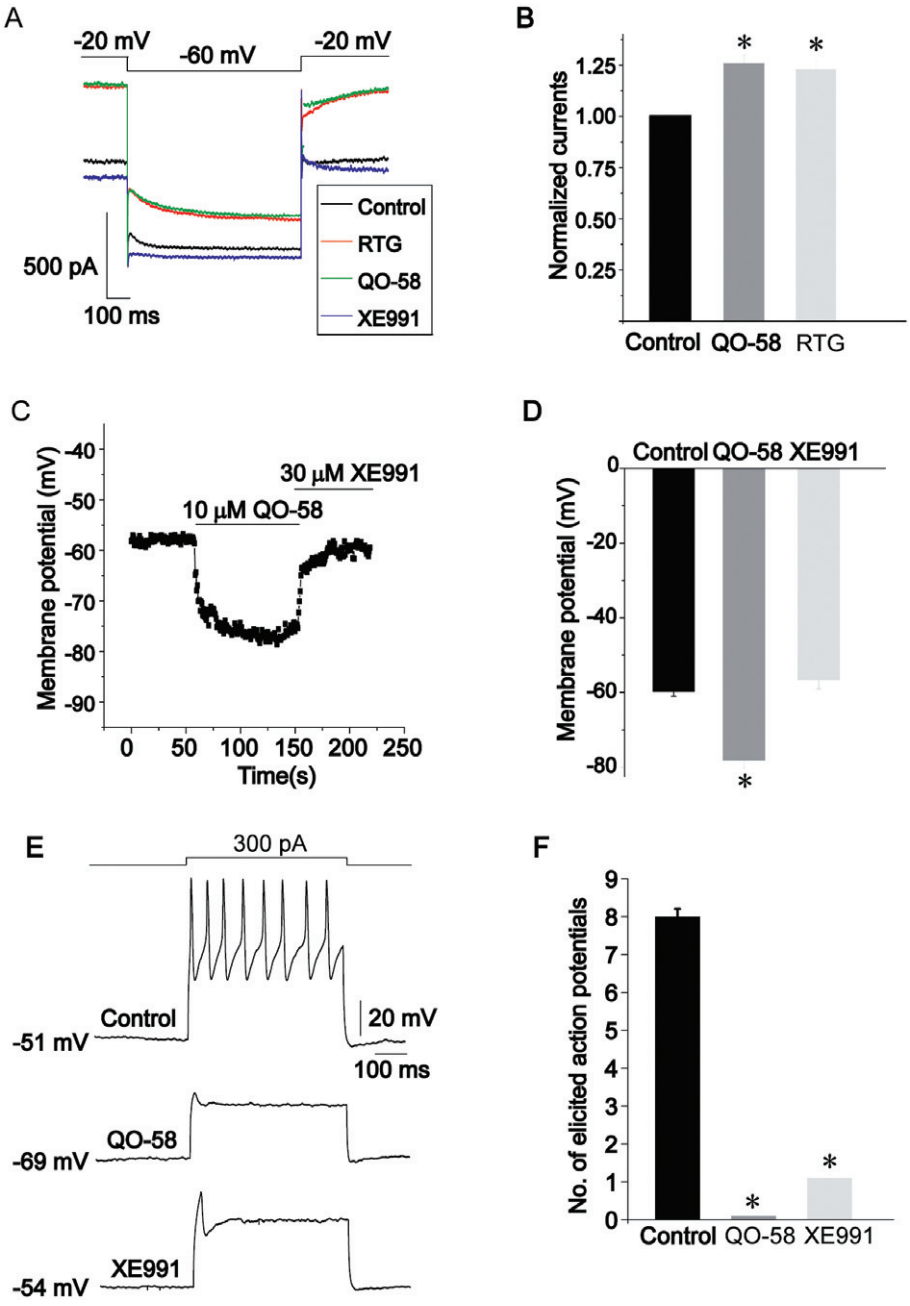

Figure 7

QO-58 enhances the M-current in DRG neurons. (A) M-current were activated at –20 mV and deactivated at –60 mV. QO-58 (10 μM) and RTG (10 μM) enhanced M-current similarly; XE991 inhibited M-current. (B) Normalized M-current amplitude in the presence of 10 μM QO-58 and 10 μM RTG (n = 5). (C) The resting membrane potential (RMP) of an isolated DRG neuron was monitored when 10 μM QO-58 was applied followed by the addition of 30 μM XE991. (D) Summary of results shown in (C): –59.7 ± 1.2 mV (control), –78.1 ± 2.3 mV (QO-58) and –56.6 ± 2.5 mV (XE991) respectively (n = 8–10). (E) Action potentials were evoked by application of a 300 pA depolarizing current. (F) Summary of results shown in (E) (n = 3). *P < 0.05.

(A306T) and K_v7.2 (L275A) reduced the efficacy of QO-58 to activate K_v7.2. QO-58 may interact with regions involving Ala^{306} and Leu^{275} of K_v7.2 to activate K_v7 channels.

In some aspects, QO-58 affected K_v7 currents similarly to a recently reported opener of K_v7 channels, ZTZ240 (Gao *et al.*, 2010). The major effects of ZTZ240 on K_v7 include hyperpolarization of voltage-dependent activation and a marked slowing of channel deactivation, which are the characteristics of QO-58's actions. Furthermore, like QO-58, ZTZ240 does not activate K_v7 through the sites used by RTG, and interestingly, Ala^{309} is important for the effects of ZTZ240 whereas Ala^{306} seems to be important for the effect of QO-58; Ala^{306} and Ala^{309} are neighbouring amino acids. However, there are several differences between QO-58 and ZTZ240

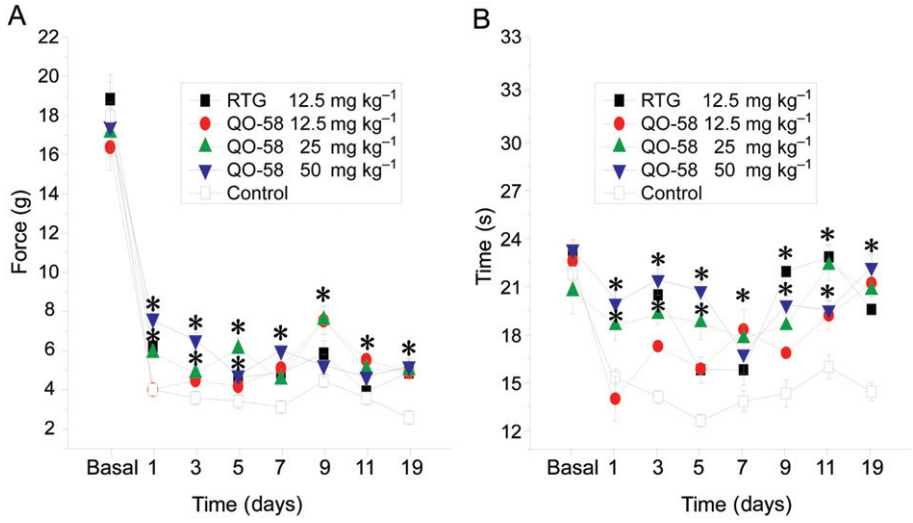

Figure 8

The effect of QO-58 on nociceptive behaviour induced by CCI of sciatic nerve. (A) Dose-dependent effect of QO-58 and RTG on withdrawal threshold to mechanical stimulus. (B) Dose-dependent effect of QO-58 and RTG on withdrawal time in response to radiant thermal stimulus. n = 6–8 rats per group, $^*P < 0.05$.

regarding their effects on K_v7 channels: firstly, QO-58 but not ZTZ240 activated the $K_v7.1$ channel. Secondly, compared with ZTZ240, QO-58 has a more selective effect on $K_v7.4$.

The CCI of a peripheral nerve is a widely used experimental model for neuropathic pain. In this study, we found that QO-58, as well as RTG, significantly reduced the nociceptive responses to mechanical and thermal stimuli in CCI rats, which suggests these K^+ channel openers have the potential to be developed further for treatment of neuropathic pain.

Acknowledgements

This work was supported by the National Natural Science Foundation of China (30730031 to H.L.Z., 30500112 to X.N.D.), the National Basic Research Program (2007CB512100) and a National 863 project (2006AA02Z183 to H.L.Z.). The Hebei Provincial Natural Science Foundation of China (C2011206021 to Y.M.) is also acknowledged. We thank Bo Qiu and Liman Huo for their kind help.

Conflict of interest

There are no conflicts of interest.

References

Alexander SP, Mathie A, Peters JA (2011). Guide to receptors and channels (GRAC), 5th edn. Br J Pharmacol 164 (Suppl. 1): S1–S324.

Blackburn-Munro G, Jensen BS (2003). The anticonvulsant retigabine attenuates nociceptive behaviours in rat models of persistent and neuropathic pain. Eur J Pharmacol 460: 109–116.

Brueggemann LI, Mackie AR, Martin JL, Cribbs LL, Byron KL (2011). Diclofenac distinguishes among homomeric and heteromeric potassium channels composed of KCNQ4 and KCNQ5 subunits. Mol Pharmacol 79: 10–23.

Chaplan SR, Bach FW, Pogrel JW, Chung JM, Yaksh TL (1994). Quantitative assessment of tactile allodynia in the rat paw. J Neurosci Methods 53: 55–63.

Coppola G, Castaldo P, Miraglia del Giudice E, Bellini G, Galasso F, Soldovieri MV *et al.* (2003). A novel KCNQ2 K^+ channel mutation in benign neonatal convulsions and centrotemporal spikes. Neurology 61: 131–134.

Dedek K, Kunath B, Kananura C, Reuner U, Jentsch TJ, Steinlein OK (2001). Myokymia and neonatal epilepsy caused by a mutation in the voltage sensor of the KCNQ2 K^+ channel. Proc Natl Acad Sci U S A 98: 12272–12277.

Devulder J (2010). Flupirtine in pain management: pharmacological properties and clinical use. CNS Drugs 24: 867–881.

Du XN, Zhang X, Qi JL, An HL, Li JW, Wan YM *et al.* (2011). Characteristics and molecular basis of celecoxib modulation on K(v)7 potassium channels. Br J Pharmacol 164: 1722–1737.

Fattore C, Perucca E (2011). Novel medications for epilepsy. Drugs 71: 2151–2178.

Gao Z, Zhang T, Wu M, Xiong Q, Sun H, Zhang Y *et al.* (2010). Isoform-specific prolongation of Kv7 (KCNQ) potassium channel opening mediated by new molecular determinants for drug-channel interactions. J Biol Chem 285: 28322–28332.

Hargreaves K, Dubner R, Brown F, Flores C, Joris J (1988). A new and sensitive method for measuring thermal nociception in cutaneous hyperalgesia. Pain 32: 77–88.

Hu H, Vervaeke K, Storm JF (2007). M-channels (Kv7/KCNQ channels) that regulate synaptic integration, excitability, and spike pattern of CA1 pyramidal cells are located in the perisomatic region. J Neurosci 27: 1853–1867.

Jia C, Qi J, Zhang F, Mi Y, Zhang X, Chen X *et al.* (2011). Activation of KCNQ2/3 potassium channels by novel pyrazolo[1,5-a]pyrimidin-7(4H)-one derivatives. Pharmacology 87: 297–310.

Kapetanovic IM, Yonekawa WD, Kupferberg HJ (1995). The effects of D-23129, a new experimental anticonvulsant drug, on neurotransmitter amino acids in the rat hippocampus in vitro. Epilepsy Res 22: 167–173.

Kilkenny C, Browne W, Cuthill IC, Emerson M, Altman DG (2010). NC3Rs Reporting Guidelines Working Group. Br J Pharmacol 160: 1577–1579.

Linley JE, Rose K, Patil M, Robertson B, Akopian AN, Gamper N (2008). Inhibition of M current in sensory neurons by exogenous proteases: a signaling pathway mediating inflammatory nociception. J Neurosci 28: 11240–11249.

Liu B, Zhang X, Wang C, Zhang G, Zhang H (2008). Antihistamine mepyramine directly inhibits KCNQ/M channel and depolarizes rat superior cervical ganglion neurons. Neuropharmacology 54: 629–639.

McGrath J, Drummond G, McLachlan E, Kilkenny C, Wainwright C (2010). Guidelines for reporting experiments involving animals: the ARRIVE guidelines. Br J Pharmacol 160: 1573–1576.

Miceli F, Soldovieri MV, Martire M, Taglialatela M (2008). Molecular pharmacology and therapeutic potential of neuronal Kv7-modulating drugs. Curr Opin Pharmacol 8: 65–74.

Munro G, Dalby-Brown W (2007). Kv7 (KCNQ) channel modulators and neuropathic pain. J Med Chem 50: 2576–2582.

Ng FL, Davis AJ, Jepps TA, Harhun MI, Yeung SY, Wan A *et al.* (2011). Expression and function of the K^+ channel KCNQ genes in human arteries. Br J Pharmacol 162: 42–53.

Peretz A, Degani N, Nachman R, Uziyel Y, Gibor G, Shabat D *et al.* (2005). Meclofenamic acid and diclofenac, novel templates of KCNQ2/Q3 potassium channel openers, depress cortical neuron activity and exhibit anticonvulsant properties. Mol Pharmacol 67: 1053–1066.

Peretz A, Sheinin A, Yue C, Degani-Katzav N, Gibor G, Nachman R *et al.* (2007). Pre- and postsynaptic activation of M-channels by a novel opener dampens neuronal firing and transmitter release. J Neurophysiol 97: 283–295.

Peretz A, Pell L, Gofman Y, Haitin Y, Shamgar L, Patrich E *et al.* (2010). Targeting the voltage sensor of Kv7.2 voltage-gated K^+ channels with a new gating-modifier. Proc Natl Acad Sci U S A 107: 15637–15642.

Qi J, Zhang F, Mi Y, Fu Y, Xu W, Zhang D *et al.* (2011). Design, synthesis and biological activity of pyrazolo[1,5-a]pyrimidin-7(4H)-ones as novel Kv7/KCNQ potassium channel activators. Eur J Med Chem 46: 934–943.

Rose K, Ooi L, Dalle C, Robertson B, Wood IC, Gamper N (2011). Transcriptional repression of the M channel subunit Kv7.2 in chronic nerve injury. Pain 152: 742–754.

Shah MM, Mistry M, Marsh SJ, Brown DA, Delmas P (2002). Molecular correlates of the M-current in cultured rat hippocampal neurons. J Physiol 544 (Pt 1): 29–37.

Sommer C, Schafers M (1998). Painful mononeuropathy in C57BL/Wld mice with delayed wallerian degeneration: differential effects of cytokine production and nerve regeneration on thermal and mechanical hypersensitivity. Brain Res 784: 154–162.

Tatulian L, Delmas P, Abogadie FC, Brown DA (2001). Activation of expressed KCNQ potassium currents and native neuronal M-type potassium currents by the anti-convulsant drug retigabine. J Neurosci 21: 5535–5545.

Wang HS, Pan Z, Shi W, Brown BS, Wymore RS, Cohen IS *et al.* (1998). KCNQ2 and KCNQ3 potassium channel subunits: molecular correlates of the M-channel. Science 282: 1890–1893.

Weisenberg JL, Wong M (2011). Profile of ezogabine (retigabine) and its potential as an adjunctive treatment for patients with partial-onset seizures. Neuropsychiatr Dis Treat 7: 409–414.

Wuttke TV, Seebohm G, Bail S, Maljevic S, Lerche H (2005). The new anticonvulsant retigabine favors voltage-dependent opening of the Kv7.2 (KCNQ2) channel by binding to its activation gate. Mol Pharmacol 67: 1009–1017.

Wuttke TV, Jurkat-Rott K, Paulus W, Garncarek M, Lehmann-Horn F, Lerche H (2007). Peripheral nerve hyperexcitability due to dominant-negative KCNQ2 mutations. Neurology 69: 2045–2053.

Xiong Q, Sun H, Li M (2007). Zinc pyrithione-mediated activation of voltage-gated KCNQ potassium channels rescues epileptogenic mutants. Nat Chem Biol 3: 287–296.

Xiong Q, Gao Z, Wang W, Li M (2008). Activation of Kv7 (KCNQ) voltage-gated potassium channels by synthetic compounds. Trends Pharmacol Sci 29: 99–107.

Yoshida S, Matsumoto S (2005). Effects of alpha-dendrotoxin on K^+ currents and action potentials in tetrodotoxin-resistant adult rat trigeminal ganglion neurons. J Pharmacol Exp Ther 314: 437–445.

Zhou XH, Ma AQ, Liu XH, Huang C, Zhang YM, Shi RM (2006). A novel mutation in KCNQ2 gene causes benign familial infantile convulsions (BFIC) in a Chinese family. Zhonghua Er Ke Za Zhi 44: 487–491.

Supporting information

Additional Supporting Information may be found in the online version of this article:

Figure S1 The effect of QO-58 on the activation and deactivation kinetics of K_v7 channel currents. The left panel shows the effects of QO-58 (10 μM) on the activation and deactivation kinetics of K_v7 currents. The right panel shows the summarized data of the activation and deactivation time constants of K_v7 currents (n = 4–6, $^*P < 0.05$).

Figure S2 Docking results for the interaction of QO-58 with residues within S5 and S6 of the $K_v7.2$ channel. The open (A and B) and the closed (C) conformations of S5 and S6 segments with the pore loop were shown. (D) The 3D structure of compound QO-58. D shows the hydrogen bonds (blue dotted lines) between QO-58. Residues Leu272 and Leu275 are shown in red and yellow colours respectively.

Figure S3 The effects of QO-58 on wild-type $K_v7.2$, $K_v7.2$ (A306T), $K_v7.2$ (L275A) currents. (A,C,E) The currents were recorded using the voltage protocol shown in Figure 6 in the absence and presence of 10 μM QO-58. (B,D,F) The change of $V_{1/2}$ from –46.3 ± 1.2 mV to –74.8 ± 2.8 mV was seen for $K_v7.2$ (A306) and from –30.2 ± 1.9 mV to –67.5 ± 3.5 mV for $K_v7.2$ (L275A) (n = 4–6, $^*P < 0.05$).

Figure S4 The effects of QO-58 on BFNC mutant channel currents. (A) The $K_v7.2$ (R207W) and $K_v7.2$ (Y284C) channel currents were recorded in the absence and presence of 10 μM QO-58 using the voltage protocol holding at –80 mV, in 10 mV incremental voltage steps from –70 to +50 mV. (B) Histogram plotting of the QO-58 effect on $K_v7.2$ (R207W) and $K_v7.2$ (Y284C) channel currents generated by step depolarization at –40 mV and at +30 mV (n = 3–4, $^*P < 0.05$).